

Fermiology and superconductivity studies on the non-tetrachalcogenafulvalene structured organic superconductor β -(BDA-TTP)₂SbF₆

E. S. Choi, E. Jobilong, A. Wade, E. Goetz, J. S. Brooks

National High Magnetic Field Laboratory, Florida State University, Tallahassee, Florida 32310

J. Yamada

*Department of Material Science, Faculty of Science,
Himeji Institute of Technology, Hyogo 678-1297, Japan,*

T. Mizutani, T. Kinoshita, M. Tokumoto

Nanotechnology Research Institute, Natl Inst. of Advanced Industrial Science and Technology, Ibaraki 305-8568, Japan

The quantum oscillatory effect and superconductivity in a non-tetrachalcogenafulvalene (TCF) structure based organic superconductor β -(BDA-TTP)₂SbF₆ are studied. Here the Shubnikov-de Haas effect (SdH) and angular dependent magnetoresistance oscillations (AMRO) are observed. The oscillation frequency associated with a cylindrical Fermi surface is found to be about 4050 tesla, which is also verified by the tunnel diode oscillator (TDO) measurement. The upper critical field (H_{c2}) measurement in a tilted magnetic field and the TDO measurement in the mixed state reveal a highly anisotropic superconducting nature in this material. We compared physical properties of β -(BDA-TTP)₂SbF₆ with typical TCF structure based quasi two-dimensional organic conductors. A notable feature of β -(BDA-TTP)₂SbF₆ superconductor is a large value of effective cyclotron mass $m_c^* = 12.4 \pm 1.1 m_e$, which is the largest yet found in an organic superconductor. A possible origin of the enhanced effective mass and its relation to the superconductivity are briefly discussed.

I. INTRODUCTION

Recent synthesis of new organic superconductors β -(BDA-TTP)₂X (where BDA-TTP is 2,5-bis(1,3-dithian-2-ylidene)-1,3,4,6-tetrathiapentalene and $X^- = \text{SbF}_6^-$, AsF_6^- and PF_6^-) has attracted interest because the π -electron donor molecules have a unique structure.¹ Most charge transfer salt organic superconductors have π -electron donors with tetrachalcogenafulvalene (TCF) structures, but BDA-TTP is the derivative of BM-TTP (2,5-bis(methylene)-1,3,4,6-tetrathiapentalene) whose structure is different as shown in Fig. 1(a). Though the π -electron overlapping along the donor-stacking directions is known to play an important role in the superconductivity as well as metallic properties in organic conductors, the detailed mechanism is not yet well understood.² Since the electron-molecular-vibration (EMV) coupling will be different between TCF and BM-TTP structured molecules, they provide new materials for comparative studies.

The superconductivity of β -(BDA-TTP)₂SbF₆ ($T_c \approx 6.5$ K) was characterized from the temperature dependence of the upper critical field H_{c2} and the specific heat measurement by Shimojo et al.³ The overall properties were found to be similar to those of the other layered organic superconductors. The specific heat jump at superconducting transition is about $\Delta C_e / \gamma T_c = 1.1$, which is smaller than the value 1.43 for weak-coupling BCS superconductor. However, the quantum oscillatory effects, which are powerful tools for determining the electronic structure of organic conductors, have not previously been reported. According to a tight binding band calculation result, a nearly isotropic cylindrical Fermi surface exists

as shown in Fig. 1(b), which is characteristic to β -type organic conductors.¹

In this paper, we report the first observation of Shubnikov-de Haas (SdH) effect and the angular-dependent magnetoresistance oscillations (AMRO) of β -(BDA-TTP)₂SbF₆ superconductor. We also performed a tunnel diode oscillator (TDO) measurement on the same material and observed quantum oscillations corresponding to the cylindrical Fermi surface. The measured frequency of SdH oscillation is in good agreement with the band calculation result. Superconducting properties are studied by the angular dependent H_{c2} and TDO measurements. Finally, fermiological and superconducting properties based on this work and previous reports are compared to other organic superconductors.

II. EXPERIMENTAL DETAILS

Single crystal samples were prepared by typical electrochemical technique.¹ For the magnetoresistance measurement, the four probe method was employed with low frequency lock-in techniques. Four gold wires were attached to a plate-like samples using graphite paint, and typically 10 μA current was applied perpendicular to the conducting planes (ac -plane). The samples were mounted on a rotator probe of a dilution refrigerator, which is situated in a 33 tesla resistive magnet at the National High Magnetic Field Laboratory, Tallahassee. The contact configuration and the definition of rotation angle are shown in Fig. 1(c).

For the TDO measurement, a sample with dimensions $1.7 \times 1.1 \times 3.1 \text{ mm}^3$ was placed inside a solenoid which

is a part of a LC tank circuit. The filling factor of the solenoid is about 0.17 and the solenoid and sample was oriented such that conducting planes are perpendicular to the external magnetic field and parallel to the solenoid rf field. The detailed experimental procedure is published elsewhere.⁴

III. DATA AND RESULTS

A. Quantum Oscillations

Fig. 2 shows the magnetoresistance (MR) data at different temperatures between 50 and 800 mK for the magnetic field direction perpendicular to the conducting planes. Resistance as a function of temperature at zero field, shown in the lower inset, is different from the result of Ref. 1 who reported a negative temperature coefficient of resistance (TCR) at temperatures above about 180 K. However more recent measurements³ are consistent with our observation of a positive TCR from room temperature to T_c . Although small offsets are sometimes observed in the resistance below T_c , the superconducting critical field transitions and quantum oscillations are clearly observed in MR data. H_{c2} shifts to higher field with decreasing temperatures, and an anomalous peak in MR can be seen near H_{c2} . These "hump" structures, commonly observed in some organic superconductors, will be discussed below. Only one frequency (F_α) at about 4050 tesla was obtained from the Fast Fourier Transform (FFT) as shown in the inset. The angular dependence of this frequency follows a $1/\cos\theta$ dependence, which is expected for a two dimensional (2D), cylindrical Fermi surface. The same oscillation frequency was observed in the TDO measurements, also discussed below. Neither beating behavior nor oscillations with different frequencies were observed for the angles measured.

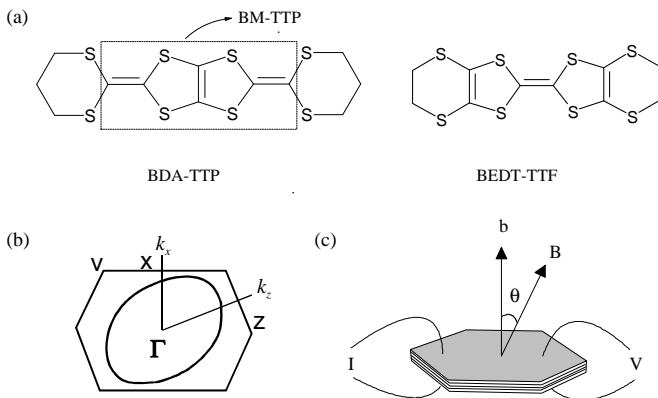


FIG. 1: (a) Donor molecular structure of BDA-TTP and BEDT-TTF. (b) Theoretical Fermi surface of β -(BDA-TTP)₂SbF₆. (c) The configuration of contacts and sample orientations for the magnetoresistance measurement.

F_α corresponds to a Fermi surface with extremal area of $3.86 \times 10^{15} \text{cm}^{-2}$, which is in good agreement with the band calculation result. The effective cyclotron mass (m_c^*) and the Dingle temperature (T_D) can be obtained by fitting the temperature and field dependence of the oscillation amplitude to the Lifshitz-Kosevich (LK) formula.⁵ According to the 2D LK formula, the amplitude (A) of fundamental oscillations can be expressed as,

$$A = \frac{\alpha m_c^* T / B}{\sinh(\alpha m_c^* T / B)} \times \exp(-\alpha m_c^* T_D / B) \times \cos\left(\frac{1}{2} \pi g m_b\right) = R_T \times R_D \times R_S, \quad (1)$$

where $\alpha = 14.69 \text{ T/K}$, m_c^* is the effective cyclotron mass, T_D is the Dingle temperature, g is the spin g -factor and m_b is the band effective mass. Each term is associated with damping effects due to finite temperature (R_T), electron scattering (R_D) and spin splitting (R_S) respectively. (When the oscillatory part of the magnetoresistance is used to determine the effective mass from R_T , it is necessary to normalize this signal by the background magnetoresistance, as we have done in the following analysis.

The results of the LK fit are shown in Fig. 3. m_c^* was estimated to be about $12.4 \pm 1.1 m_e$, which is quite large compared to other organic conductors. T_D is about 1.0 K, which corresponds to a relaxation time $\tau \approx 1.1 \times 10^{-12}$ sec and a mean free path $l \approx 795 \text{ \AA}$. Due to large m_c^* , the condition $\omega_c \tau > 1$ is satisfied when the magnetic field is larger than 64 T, which is probably why quantum oscillations were not observed at lower fields in previous work.

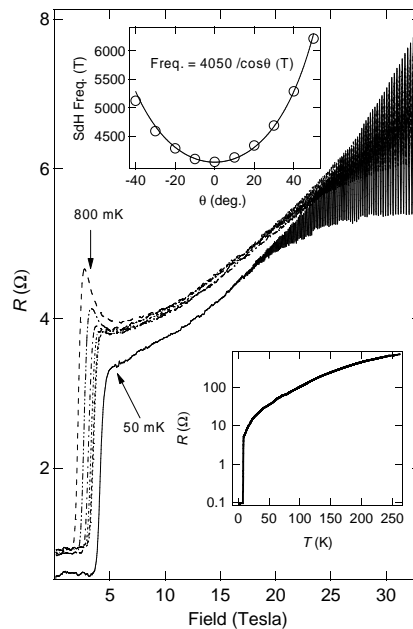


FIG. 2: Magnetoresistance of β -(BDA-TTP)₂SbF₆ at different temperatures. Insets: Resistance as a function of temperature at zero field and angular dependence of SdH oscillation frequency.

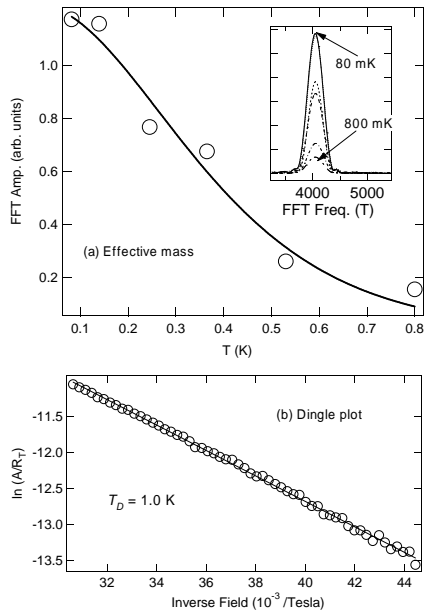


FIG. 3: (a) Effective mass fitting using the LK formula. The inset shows FFT amplitudes for different temperatures used for the effective mass fitting. (b) Dingle plot of β -(BDA-TTP)₂SbF₆

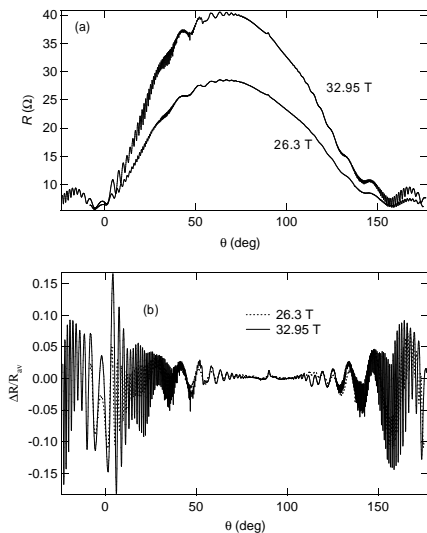


FIG. 4: (a) AMRO data at 50 mK for two different fields and (b) AMRO amplitude after subtracting background magnetoresistance.

Fig. 4(a) shows the AMRO data of β -(BDA-TTP)₂SbF₆ at 50 mK when the magnetic field is fixed at 32.95 and 26.3 tesla. The AMRO signal can be more clearly seen by subtracting the background MR as shown in Fig. 4(b). Besides the SdH oscillations for θ near 0 and 180°, additional oscillations, so called Yamaji oscillations,⁶ are clearly seen for $20^\circ \leq \theta \leq 80^\circ$ and 100°

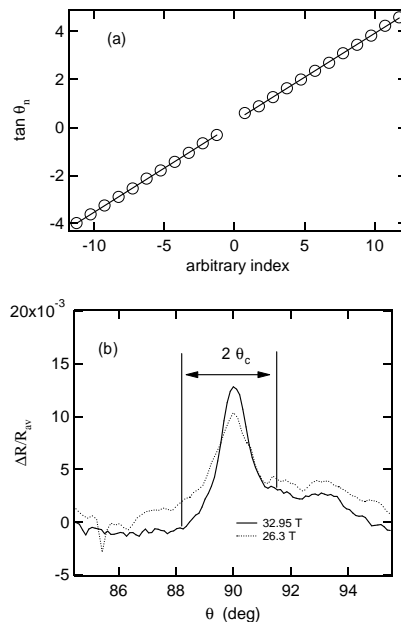


FIG. 5: (a) $\tan \theta$ plot for Yamaji oscillations. (b) Expansion of AMRO amplitude near $\theta=90^\circ$.

$\leq \theta \leq 160^\circ$. The peaks in the Yamaji oscillation are periodic in $\tan \theta$ as shown in Fig. 5(a), which indicates that the cylindrical Fermi surface is corrugated along the b^* -direction. The periodicity of $\tan \theta$ is related to the maximum Fermi wave vector projection to the field rotation plane k_F by the relation $bk_F \tan \theta = \pi(n - 1/4)$, where b is the lattice parameter along the b -axis. From the slope of Fig. 5(a), k_F is estimated to be about $4.89 \times 10^7 \text{ cm}^{-1}$, which gives cross-sectional area $\pi k_F^2 = 7.5 \times 10^{15} \text{ cm}^{-2}$, two times larger than the area from the SdH oscillation. Furthermore, the k_F values is comparable to the distance of ΓZ in the momentum space. The discrepancy of Fermi surface areas between two experimental values obtained from AMRO and SdH effect is not unusual and it can be ascribed to higher order terms of Yamaji oscillations⁷ or effective doubling of the interlayer distance⁸.

In Fig. 5(b), a peak in resistance (see also Fig. 4) near $\theta=90^\circ$ is clearly shown. A peak in AMRO for the magnetic field parallel to the conducting layers has been observed in many organic conductors, and is used as a proof of coherent interlayer transport.⁹ Other experimental results, like a beat frequency in the magnetic oscillations and a crossover from a linear to a quadratic field dependence have also been suggested as a test for coherent transport.¹⁰ However, no beating behavior was observed for our data, which may be ascribed to very small value of interlayer transfer integral (t_b) compared to the Fermi energy (ϵ_F). The ratio of the interlayer and the Fermi energy (t_b/ϵ_F) can be esti-

mated from the relation $t_b/\epsilon_F = (\pi/2 - \theta_c)/bk_F$, where θ_c is the critical angle above which the resistance increases rapidly.⁹ Using the crystallographic parameters and the experimental value of k_F obtained from the SdH oscillation, t_b/ϵ_F is estimated to be about 1/250, and 1/350 when k_F from AMRO is used. This value is comparable to β_H -(BEDT-TTF)₂I₃ (1/175) and β -(BEDT-TTF)₂IBr₂ (1/280) which both show beating behavior¹¹. Hence the reason why we do not observe a beat frequency in β -(BDA-TTP)₂SbF₆ is not clear yet.

The amplitude of SdH oscillations in AMRO data can be obtained by subtracting AMRO and background magnetoresistance. The result is shown in Fig. 6 for $H=32.95$ tesla. There are some nodes periodic in $1/\cos\theta$, which can be more clearly seen by plotting the locations of nodes and anti-nodes in $1/\cos\theta$ against odd and even integers. This behavior in AMRO can be explained by the spin splitting term R_S in Eq. 1, where $\cos(\pi gm_b/2)$ will show minima (maxima) when gm_b are odd (even) integers. Since the magnetic field is constant in AMRO measurements, the nodes come from the angular dependence of $m_b(\theta)$. In the framework of Fermi liquid theory, m_c^* can be written as $m_c^* = m_b(1+\lambda)$, where λ is the mass enhancement factor. And the angular dependence of m_c^* is known to follow $1/\cos\theta$ dependence. From the slope of $1/\cos\theta$ plot, we obtained $gm_b \sim 15.6m_e$, which is about 30% larger than the largest known value in pervious organic conductors.¹² The gm_b values for representative organic conductors are listed in Table I.

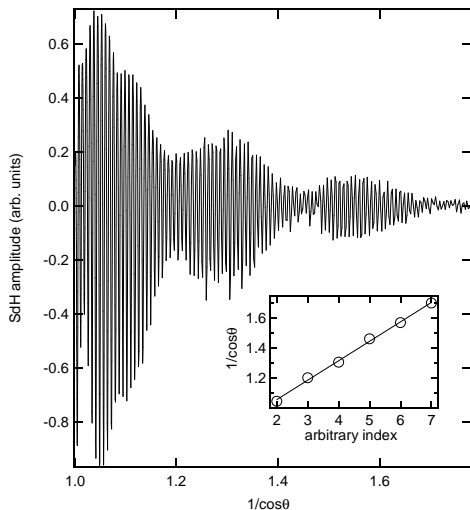


FIG. 6: (a) SdH oscillation amplitude after subtracting AMRO from the data of Fig. 4 as a function of $\cos\theta$. Inset : Positions of nodes and antinodes of SdH amplitude in $1/\cos\theta$

B. Superconductivity

Fig. 7 shows the angular dependence of $H_{c2}(\theta)$ at two different temperatures. H_{c2} was determined by the field where the first derivative of $R(H)$ shows an extremum. The values at $\theta=0$ and 90° are in good agreement with the previous report when the $H_{c2}(T)$ curves in Ref. 3 are extrapolated to lower temperatures. The solid and dashed line in Fig. 7(c) are the fitting curves for the case of a 2D film¹³ and using the 3D anisotropic GL theory¹⁴, respectively. Each can be expressed as

$$1 = \left| \frac{H_{c2}(\theta) \cos\theta}{H_{c2\perp}} \right| + \left(\frac{H_{c2}(\theta) \sin\theta}{H_{c2\parallel}} \right)^2 : 2D, \quad (2)$$

$$H_{c2}(\theta) = \frac{\phi_0}{2\pi\xi_{\parallel}^2 \sqrt{\cos^2\theta + \frac{H_{c2\perp}^2}{H_{c2\parallel}^2} \sin^2\theta}} : 3D, \quad (3)$$

where ϕ is the flux quantum and ξ is the coherence length. The validity of the application of these models depends on relative magnitude of the inter-layer coherence length (ξ_{\perp}) and inter-layer distance (b), i.e., the 2D model is more appropriate for $\xi_{\perp} < b$ and vice versa. Although both fitting curves give approximate fits to the data, the 2D model gives slightly better results. For comparison, κ -(BEDT-TTF)₂I₃ superconductors show quite satisfactory fitting results using the 2D model, and their quantum oscillation also show peculiar features which were

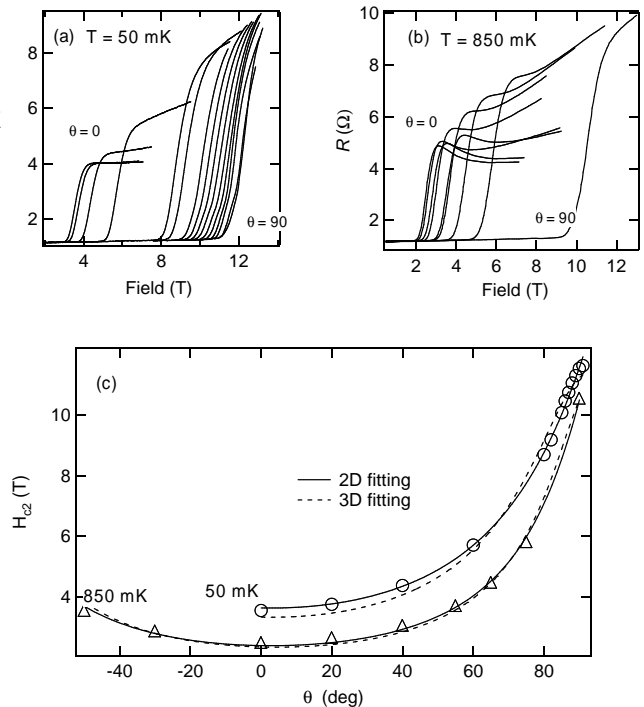


FIG. 7: (a) Magnetoresistance near H_{c2} at different angles when $T = T=50$ mK (a) and 850 mK (b) H_{c2} as a function of θ . The fitted curves for the 2D and 3D model are also shown.

ascribed to nearly perfect two-dimensionality.^{12,15} If one considers only the criterion of the two lengths, which are ξ_{\perp} (26 Å) and b (17.6 Å), the 3D model seems to be more appropriate. Nevertheless, $H_{c2}(\theta)$ is described better by the 2D formula.

The anomalous behavior in MR, a "hump" structure, near H_{c2} is also seen in Fig. 7(b). The hump structure is most significant for $\theta=0$ ($H \perp$ conducting planes) and almost disappears for $\theta = 90^{\circ}$ ($H \parallel$ conducting planes). This behavior was observed for other κ - and β'' -type organic superconductors, which share several common features.¹⁶ It is highly anisotropic for both electric current and magnetic field directions; it is most significant when the inter-plane resistance is measured with the magnetic field perpendicular to the conducting planes. And it is suppressed with decreasing temperature and increasing uniaxial stress along the inter-plane direction.¹⁷ In β -(BDA-TTP)₂SbF₆, the temperature dependence (see Fig. 2) and anisotropic features are also apparent, while the hump structure in this material can be still seen at very low temperatures down to 80 mK.

C. Tunnel Diode Oscillator Study

Fig. 8 shows the field dependence of a resonant frequency (f_r) of TDO at low field regions between 7.0 and 0.45 K. When the temperature is below T_c , the

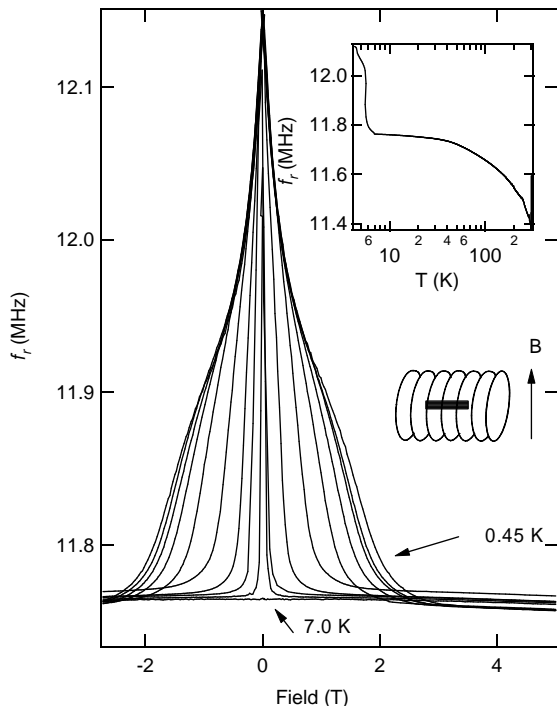


FIG. 8: TDO resonant frequency (f_r) at different temperatures. The inset shows the temperature dependence of f_r at zero field.

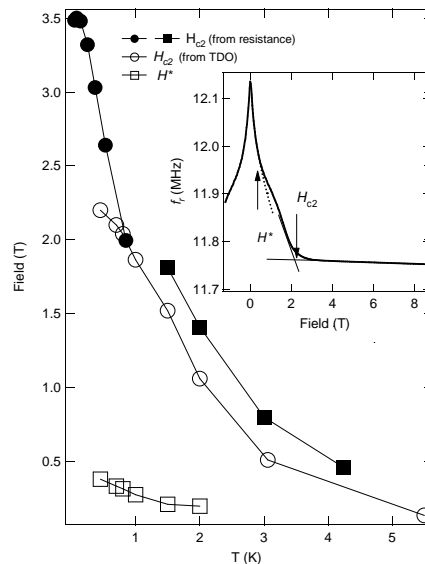


FIG. 9: T - H phase diagram based on TDO measurements and resistance measurements done two different samples. Inset : definition of H_{c2} and H^* in the TDO experiment

frequency decreases sharply with increasing field until superconducting-normal transition occurs. In the normal state, the frequency change is less significant showing gradual decrease. The difference in magnitude of the resonant frequency in the superconducting and normal state can be also seen in the zero-field cool-down curve as shown in the inset of Fig. 8. Since the resonant frequency of an LC circuit is $f_r=1/(2\pi\sqrt{LC})$, the change of f_r mainly comes from the change of inductance of the coil.

The decrease of f_r , i.e., the increase of L in superconducting-metal transitions can be ascribed to the penetration of the rf field to the sample.^{8,18} The rf field will be expelled when a sample is in the superconducting state, which results in a decrease of L and increase of f_r . Following this argument, a H - T phase diagram can be built based on the TDO experiment. H_{c2} was defined as a intersection point of extrapolations of $f_r(H)$ above and below the transition. And the field where $f_r(H)$ show change of curvatures (H^*) was defined as a point that $f_r(H)$ starts to deviate $H^{1/2}$ dependence. Our work shows similar behavior compared with the results of Ref. 8, in which H^* in λ -(BETS)₂GaCl₄ superconductor was ascribed to the change of fluxoid motion in the mixed state. According to this model, fluxoid motion can be explained by a simple harmonic oscillator when $H \ll H_{c2}$ and $H < H^*$. In this regime, the frequency change, or equivalently the penetration depth follows $H^{1/2}$ dependence. Above H^* , the deviation from the $H^{1/2}$ behavior was attributed to the flux-lattice melting, which occurs when the thermal displacement of vortex lattice becomes significant compared to lattice parameters.¹⁹

The resulting H - T phase diagram is shown in Fig. 9,

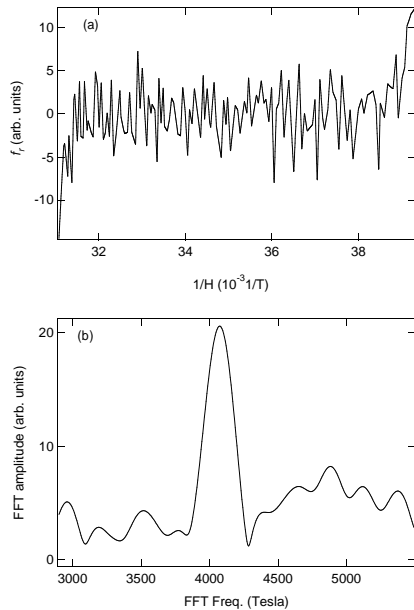


FIG. 10: TDO resonant frequency at high field region for $T=0.45$ K

where H_{c2} values from the resistance measurement on two samples are also plotted. H_{c2} values from the two different experiments overlap at $T \approx 0.8$ K, but H_{c2} values from the resistance measurement seem to show more pronounced temperature dependence at lower temperatures. The $H_{c2}(T)$ curves do not follow the power law $H_{c2} \propto (T_c - T)^n$ behavior in the whole temperature range, rather there seems to be a change of curvature around $T=2$ K.

The amplitudes of quantum oscillations of f_r in the normal state between 25 and 32 tesla is shown as a function of inverse field in Fig. 10. The overall signal to noise ratio is so small that it is difficult to resolve the nature of quantum oscillations directly from the TDO data. However, the oscillation frequency obtained from FFT is about 4070 T, very similar to that of the resistance measurement.

IV. DISCUSSION

The electronic structure and superconductivity of β -(BDA-TTP)₂SbF₆ have many common features with other organic superconductors. The molecular packing mode of this material is known to be very similar to that of β -(BEDT-TTF)₂I₃. Correspondingly, the Fermi surface of β -(BDA-TTP)₂SbF₆ resembles the other β -type organic conductors both in the band calculation and experimental results. The superconductivity in β -(BDA-TTP)₂SbF₆ also has similar characteristics to other ET and BETS organic superconductors. $H_{c2}(\theta)$ measurements revealed the anisotropic nature of the superconductivity in β -(BDA-TTP)₂SbF₆.

There could be a possibility of a dimensional crossover due to the increase of the perpendicular coherence length ξ_{\perp} at higher temperatures than $H_{c2}(\theta)$ measurements were done in this work.¹⁵ The deviation from the power law of $H_{c2}(T)$ curves could be a indication of a dimensional crossover, which was suggested for λ -(BETS)₂GaCl₄ superconductors.⁸

In Table I, we have listed some physical parameters related to fermiology and superconductivity of several organic superconductors including β -(BDA-TTP)₂SbF₆. F_{α} and $m_{c\alpha}^*$ denote the FFT frequency and effective cyclotron mass for fundamental orbits and F_{β} and $m_{c\beta}^*$ for breakdown orbits. When two orbits coexist, the value for the β -orbit is more appropriate for comparison, since it covers a larger area of the Fermi surface.

The striking difference between β -(BDA-TTP)₂SbF₆ and other organic superconductors can be found in values of m_c^* and gm_b . Since the Fermi surface of β -(BDA-TTP)₂SbF₆ is similar to other β -type organic conductors, the difference can be attributed to many body effects which are not considered in the band calculation.

In the framework of Fermi liquid theory, several effective masses can be defined.²⁰ Experimentally, SdH and dHvA effect can be used to obtain the effective cyclotron mass m_c^* which reflects mass enhancement by both electron-phonon and electron-electron interactions. The dynamic mass m_c is influenced only by electron-phonon interactions and can be measured by the cyclotron resonance experiment. The band mass m_b has similar value to the optical mass which can be obtained by the plasma frequency measurement. The Sommerfeld constant γ which can be measured from the specific heat measurement is related to the specific heat mass that is affected by both interactions. The mass enhancement of m_c^* due to electron-phonon and electron-electron interactions can be written as,

$$m_c^* = (1 + \lambda_{EP})(1 + \lambda_{EE})m_b = (1 + \lambda_{EE})m_c, \quad (4)$$

where λ_{EP} and λ_{EE} are the coupling strength of electron-phonon and electron-electron interactions respectively.

For several organic superconductors, λ_{EP} obtained from the magnitude of $\Delta C_e/\gamma T_c$ shows general tendency with respect to T_c , which is in agreement with weak and strong coupling limit of BCS theory.^{21,28} But β -(BDA-TTP)₂SbF₆ does not seem to agree with this tendency considering measured value of $\Delta C_e/\gamma T_c$ and T_c . The small value of $\Delta C_e/\gamma T_c$ of β -(BDA-TTP)₂SbF₆ suggests that it is below the weak coupling limit like α -(BEDT-TTF)₂NH₄Hg(SCN)₄, but its T_c value is between β' -(BEDT-TTF)₂SF₅CH₂CF₂SO₃ and κ -(BEDT-TTF)₂Cu(NCS)₂ which are in the range of intermediate and strong coupling limit (see Fig. 3 in Ref. 21 and Table I). This apparent discrepancy suggest that additional parameters should be considered for β -(BDA-TTP)₂SbF₆ superconductor.

Considering the large value of m_c^* of β -(BDA-TTP)₂SbF₆ which cannot be explained by λ_{EP} alone,

TABLE I: A comparison for fermiological and superconducting properties of organic superconductors

	F_α (T)	$m_{c\alpha}^*$ (m_e)	F_β (T)	$m_{c\beta}^*$ (m_e)	gm_b	γ (mJ/mol·K ²)	$\Delta C_e/\gamma T_c$	T_c (K)
β -(BDA-TTP) ₂ SbF ₆	4050	12.4			15.3	33 ³	1.1 ³	6.5
κ -(BEDT-TTF) ₂ Cu[N(CN) ₂]Br ^{21,22}	530	3.1	3790	6.6	9.85	25	2.7	11.5
κ -(BEDT-TTF) ₂ Cu(NCS) ₂ ^{24,25}	600	3.5	3920	6.5	5.2	25	2.0-2.8	10.4
β_H -(BEDT-TTF) ₂ I ₃ ^{12,26}	3730	4.2			11.96			8.1
β'' -(BEDT-TTF) ₂ SF ₅ CH ₂ CF ₂ SO ₃ ^{27,28}	200	1.9			4	18.7	2.1	5.2
λ -(BETS) ₂ GaCl ₄ ⁸	650	3.6	4030	6.3				5
κ -(BEDT-TTF) ₂ I ₃ ^{12,29}	570	1.9	3880	3.9	8.64	18.9	1.6	3.6
β -(BEDT-TTF) ₂ IBr ₂ ^{12,30}	3900	5.0			8.99			2.7
α -(BEDT-TTF) ₂ NH ₄ Hg(SCN) ₄ ^{12,31}	560	2.7			4.4	25	1.0	1.2

it is likely that electron-electron interactions play an important role in this material. The large values of gm_b and γ are also suggestive that the effective density of states (quasiparticle density of states) is large compared to other organic conductors. Indeed, the largest transfer integrals obtained from the band calculation were about half of those of κ -(BEDT-TTF)₂Cu(NCS)₂ and β -(BEDT-TTF)₂I₃,¹ which suggest that the narrower bandwidth could be the reason for the enhanced electron-electron interactions. At present, it is difficult to estimate the magnitudes of λ_{EP} and λ_{EE} until pressure and cyclotron resonance studies are carried out.

In conclusion, the new donor molecule organic superconductor β -(BDA-TTP)₂SbF₆ is found to have similar properties in the electronic structure and superconductivity to other typical organic superconductors. But the large effective mass indicates that many body effects are

significant in this material. In the context, this new type of donor molecules could be a new approach to increase T_c of organic conductors by enhanced electron-electron interactions.

Acknowledgments

This work was supported by NSF-DMR 99-71474. The National High Magnetic Field Laboratory is supported by a contractual agreement between the National Science Foundation and the State of Florida. A. Wade and E. Goetz were supported by REU fellowships through the Department of Physics (FSU) and the National Science Foundation(NHMFL) respectively.

-
- ¹ J. Yamada, M. Watanabe, H. Akutsu, S. Nakatsuji, H. Nishikawa, I. Ikemoto, K. Kikuchi, J. Am. Chem. Soc. **123**, 4174 (2001).
- ² T. Ishiguro, K. Yamaji and G. Saito, *Organic superconductors*, Springer-Verlag (1998).
- ³ Y. Shimojo, T. Ishiguro, T. Toita and J. Yamada, J. Phys. Soc. Japan. **71** 717 (2002)
- ⁴ G. J. Athas, J. S. Brooks, S. J. Klepper, S. Uji and M. Tokumoto, Rev. Sci. Instrum. **64** 3248 (1993).
- ⁵ I. M. Lifshitz and A. M. Kosevich, Zh. Éksp. Teor. Fiz. **29**, 730 (1955) [Soviet Physics JETP **2**, 636 (1957)].
- ⁶ K. Yamaji, J. Phys. Soc. Japan, **58** 1520 (1989).
- ⁷ S. Uji, H. Shinagawa, C. Terakura, T. Terashima, T. Yakabe, Y. Terai, M. Tokumoto, A. Kobayashi, H. Tanaka and H. Kobayashi, Phys. Rev. B **64** 024531 (2001).
- ⁸ C. H. Mielke, J. Singleton, M-S. Nam, N. Harrison, C. C. Agosta, B. Fravel and L. K. Montgomery, J. Phys.: Condens Matter. **13** 8325 (2001)
- ⁹ N. Hanasaki, S. Kagoshima, T. Hasegawa, T. Osada, N. Miura, Phys. Rev. B **57** 1336 (1998).
- ¹⁰ P. Moses, R. H. McKenzie, Phys. Rev. B **60** 7998 (1999).
- ¹¹ J. Wosnitza, G. Goll, D. Beckmann, S. Wanka, D. Schweitzer and W. Strunz, J. Phys. I **6**, 1597 (1996).
- ¹² J. Wosnitza, *Fermi Surfaces of Low-Dimensional Organic Metals and Superconductors*, Springer Verlag, Berlin-Heidelberg 1996.
- ¹³ M. Tinkham *Introduction to Superconductivity*, McGraw-Hill (1975)
- ¹⁴ R. C. Moris, R. V. Coleman and R. Bhandari, Phys. Rev. B **5**, 895 (1972).
- ¹⁵ S. Wanka, D. Beckmann, J. Wosnitza, E. Balthes, D. Schweitzer, W. Strunz and H. J. Keller, Phys. Rev. B **53** 9301 (1996).
- ¹⁶ F. Zuo, J. A. Schlueter and J. M. Williams, Phys. Rev. B **60** 574 (1999) and references therein.
- ¹⁷ E. S. Choi, J. S. Brooks, L. Balicas, S. Y. Han and J. S. Qualls, Philos. Mag. B **81** 399 (2001).
- ¹⁸ D. -H. Wu and S. Sridhar, Phys. Rev. Lett., **65** 2074 (1990).
- ¹⁹ A. Houghton, R. A. Pelcovits and A. Sudbo, Phys. Rev. B **40** 6763 (1989).
- ²⁰ J. Merino, R. H. McKenzie, Phys. Rev. B **62** 2416 (2000).
- ²¹ H. Elsinger, J. Wosnitza, S. Wanka, J. Hagel, D. Schweitzer and W. Strunz, Phys. Rev. Lett. **84** 6098 (2000).
- ²² H. Weiss, M. V. Kartsovnik, W. Biberacher, E. Balthes, A. G. M. Jansen and N. D. Kushch, Phys. Rev. B **60** R16259 (1999).
- ²³ J. Müller, M. Lang, R. Helfrich, F. Steglich and T. Sasaki,

- Phys. Rev. B **65** R140509 (2002).
- ²⁴ J. Caulfield, W. Lubczynski, F. L. Pratt, J. Singleton, D. Y. K. Ko, W. Hayes, M. Kurmoo and P. Day, J. Phys.: Condens. Matter **6** 2911 (1994).
- ²⁵ B. Andraka, J. S. Kim, G. R. Stewart, K. D. Carlson, H. H. Wang and J. M. Williams, Phys. Rev. B **40** 11345 (1989).
- ²⁶ W. Kang, G. Montambaux, J. R. Cooper, D. Jerome, P. Batail and C. Lenoir, Phys. Rev. Lett. **62** 2559 (1989).
- ²⁷ J. Wosnitza, G. Goll, D. Beckmann, S. wanka, J. A. Schlueter, J. M. Williams, P. G. Nixon, R. W. Winter and G. L. Gard, Physica B **246-247** 104 (1998).
- ²⁸ S. Wanka, J. Hagel, D. Beckmann, J. Wosnitza, J. A. Schlueter, J. M. Williams, P. G. Nixon, R. W. Winter and G. L. Gard, Phys. Rev. B **57**, 3084 (1998).
- ²⁹ J. Wosnitza, X. Liu, D. Schweitzer and H. J. Keller, Phys. Rev. B **50** 12747 (1994).
- ³⁰ M. V. Kartsovnik, V. L. Laukhin, S. I. Pesotskii, I. F. Schegolev and V. M. Yakovenko, J. Phys. I **2** 89 (1991).
- ³¹ J. Wosnitza, G. W. Crabtree, H. H. Wang, K. D. Carlson, M. D. Vashon and J. M. Williams, Phys. Rev. Lett. **67** 263 (1991).
- ³² C. H. Mielke, N. Harrison, D. G. Rickel, A. H. Lacerda, R. M. Vestal and L. K. Montgomery, Phys. Rev. B **56** R4309 (1997).
- ³³ J. Wosnitza, G. W. Crabtree, H. H. Wang, U. Geiser, J. M. Williams, K. D. Carlson, Phys. Rev. B **45** 3018 (1992).
- ³⁴ K. F. Quader, K. S. Bedell and G. E. Brown, Phys. Rev. B **36**, 156 (1987).
- ³⁵ J. Wosnitza, G. W. Crabtree, K. D. Carlson, H. H. Wang and J. M. Williams **194-196** 2007 (1994).